SMC-TR-98-21

AEROSPACE REPORT NO.
TR-93(3940)-5

# Observation of Single Event Upsets in Analog Microcircuits

15 January 1998

Prepared by

R. KOGA, S. D. PINKERTON, S. C. MOSS,
D. C. MAYER, S. LaLUMONDIERE, S. J. HANSEL,
K. B. CRAWFORD, and W. R. CRAIN
Technology Operations

Prepared for

SPACE AND MISSILE SYSTEMS CENTER
AIR FORCE MATERIEL COMMAND
2430 E. El Segundo Boulevard
Los Angeles Air Force Base, CA 90245



Engineering and Technology Group

APPROVED FOR PUBLIC RELEASE;
DISTRIBUTION UNLIMITED

THE AEROSPACE
CORPORATION
El Segundo, California

This report was submitted by The Aerospace Corporation, El Segundo, CA 90245-4691, under Contract No. F04701-93-C-0094 with the Space and Missile Systems Center, 2430 E. El Segundo Blvd., Suite 6037, Los Angeles AFB, CA 90245-4687. It was reviewed and approved for The Aerospace Corporation by A. B. Christensen, Principal Director, Space and Environment Technology Center. Maj. J. W. Cole was the project officer for the Mission-Oriented Investigation and Experimentation Program (MOIE) program.

This report has been reviewed by the Public Affairs Office (PAS) and is releasable to the National Technical Information Service (NTIS). At NTIS, it will be available to the general public, including foreign nationals.

This technical report has been reviewed and is approved for publication. Publication of this report does not constitute Air Force approval of the report's findings or conclusions. It is published only for the exchange and stimulation of ideas.

J. W. Cole, MAJ, USAF

J. W. Cole, Maj. USAF
SMC/AXES

# REPORT DOCUMENTATION PAGE

*Form Approved*
*OMB No. 0704-0188*



1. AGENCY USE ONLY (*Leave blank*)

2. REPORT DATE
15 January 1998

3. REPORT TYPE AND DATES COVERED

4. TITLE AND SUBTITLE
Observation of Single Event Upsets in Analog Microcircuits

5. FUNDING NUMBERS
F04701-93-C-0094

6. AUTHOR(S)
Koga, R.; Pinkerton, S.D.; Moss, S.C.; Mayer, D.C.,
LaLumondiere,S; Hansel, S.J.; Crawford, K.B.; and Crain, W.R.

7. PERFORMING ORGANIZATION NAME(S) AND ADDRESS(ES)
The Aerospace Corporation
Technology Operations
El Segundo, CA 90245-4691

8. PERFORMING ORGANIZATION REPORT NUMBER
TR-93(3940)-5

9. SPONSORING/MONITORING AGENCY NAME(S) AND ADDRESS(ES)
Space and Missile Systems Center
Air Force Materiel Command
2430 E. El Segundo Blvd.
Los Angeles Air Force Base, CA 90245

10. SPONSORING/MONITORING AGENCY REPORT NUMBER
SMC-TR-98-21

11. SUPPLEMENTARY NOTES

12a. DISTRIBUTION/AVAILABILITY STATEMENT
Approved for public release; distribution unlimited

12b. DISTRIBUTION CODE

13. ABSTRACT (*Maximum 200 words*)

Selected analog devices were tested for heavy ion induced single event upset (SEU). The results of these tests are presented, likely upset mechanisms are discussed, and standards for the characterization of analog upsets are suggested. The OP-15 operational amplifier, which was found to be susceptible to SEU in the laboratory, has also experienced upset in space. Possible strategies for mitigating the occurrence of analog SEUs in space are discussed.

14. SUBJECT TERMS
Analog microcircuits in space
Field effect transistor upset
Heavy ion irradiation effects
Latchup
Radiation effects
Radiation effects in space
Single event effects
Single event upset

15. NUMBER OF PAGES
11

16. PRICE CODE

| 17. SECURITY CLASSIFICATION OF REPORT | 18. SECURITY CLASSIFICATION OF THIS PAGE | 19. SECURITY CLASSIFICATION OF ABSTRACT | 20. LIMITATION OF ABSTRACT |
|---|---|---|---|
| Unclassified | Unclassified | Unclassified | |

# Observation of Single Event Upsets in Analog Microcircuits

R. Koga, S.D. Pinkerton, S.C. Moss, D.C. Mayer, S. LaLumondiere,
S.J. Hansel, K.B. Crawford, and W.R. Crain
The Aerospace Corporation
PO Box 92957, Los Angeles, CA 90009

***Abstract*** Selected analog devices were tested for heavy ion induced single event upset (SEU). The results of these tests are presented, likely upset mechanisms are discussed, and standards for the characterization of analog upsets are suggested. The OP-15 operational amplifier, which was found to be susceptible to SEU in the laboratory, has also experienced upset in space. Possible strategies for mitigating the occurrence of analog SEUs in space are discussed.

## Introduction

Heavy ions can penetrate the sensitive regions of space-borne analog microcircuits. In some circuits, the generated mobile charge creates a voltage shift at a node which may be amplified many times (e.g., within an operational amplifier), yielding a large deviation in the device output voltage. Recent results obtained in our laboratory indicate that the duration of the disturbance can be as long as a few microseconds and that the output signal swing can be substantial. This disturbance can affect circuits connected to the output of the analog microcircuit. For example, the output of an operational amplifier may be connected to the input of a digital counter that is incremented by each output pulse of the amplifier having sufficiently large amplitude (i.e., above some threshold). At that time, the disturbance is recorded as a logic state upset – a long-lasting signal – and is no longer a short transient. This type of SEU induced anomaly has recurred in the OP-15 operational amplifiers in the Earth Sensor of NASA's TOPEX satellite since it was launched into orbit in August, 1992 [1].

Over the years, single event upset (SEU) studies have been carried out for a number of digital microcircuits, such as shift registers and random access memories. However, the physics of charge generation, transport, and collection applies equally well to analog devices. It is therefore reasonable to likewise refer to an upset observed in an analog circuit as an SEU. While such analog SEUs are normally short-lived, they can leave more permanent traces in the digital circuits connected to them, as noted above.

We have conducted SEU tests of several analog device types using the heavy ions available at the Lawrence Berkeley Laboratory 88-inch cyclotron facility. The test devices, methods, and results of our studies are presented below, together with a discussion of likely upset mechanisms and possible preventative measures. Since SEUs in analog and digital devices are not strictly comparable, standards for characterizing analog SEUs will need to be developed to facilitate comparisons between different devices. In the discussion we propose a set of measurements that we believe satisfies the minimal requirement for characterizing SEUs in analog devices.

## Test Devices

The test device types (see Table 1) were selected from among the general analog microcircuits commonly used in various space systems. All the test devices have multiple difference-amplifier stages, which tend to amplify the deposited charge. As an example, the circuit diagram of the OP-15 operational amplifier is shown in Fig. 1. The first stage of the operational

Table 1. Test Devices

| Device ID | Manufacturer | Function | Lot DC | Bias† |
|---|---|---|---|---|
| HS3530RH | Harris | Operational Amplifier | 8839 | 3 to 15 |
| OP-05 | PMI* | Operational Amplifier | 9206 | 3 to 22 |
| OP-15 | PMI | Operational Amplifier | 9240 | 3 to 22 |
| LM111H | National | Voltage Comparator | 9151 | 5 to 15 |

† The nominal bias voltage range (±5 to ±15 volts) may be exceeded to the range shown here in some cases. Only unsigned numbers are shown in the table.

* Precision Monolithics Inc.

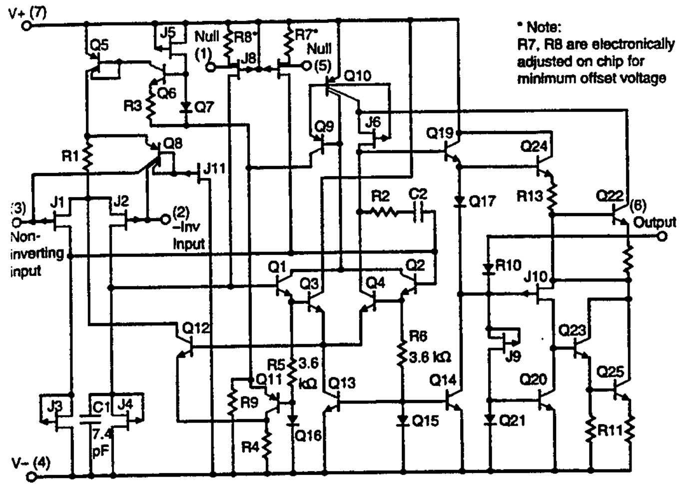


Fig. 1. Circuit schematic for OP-15
The JFET section consists of eleven transistors (J1 - J11). The remaining transistors are bipolar.

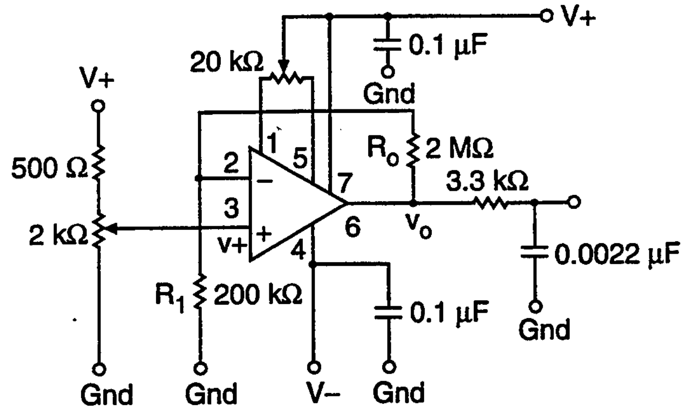


$$\frac{V_o}{V_+} = \frac{R_o + R_1}{R_1}$$

Fig. 2. Test circuit for OP-15 op amp

amplifier consists of a difference-amplifier made up of junction field-effect transistors (JFETs). The OP-05 operational amplifier is similar to the OP-15 except that it is several times slower. HS3530RH is a radiation hardened, low power, programmable operational amplifier. By selecting an appropriate set current [which can be controlled by the voltage applied to pin 8 via the equation, $V_{set}$ (volts) = $1 \times 10^{-5}$ $I_{set}$ (amp)], various internal operating characteristics can be adjusted, such as power dissipation, gain-bandwidth product, open loop gain, and slew rate. According to the manufacturer's specifications, these characteristics should remain constant over a voltage supply range of +3 V to +15 V. LM111H is a voltage comparator that is designed to operate over a wide range of supply voltages (from standard ±15 V to a single +5 V supply). Detailed information on the test devices is available from the respective manufacturers.

We did not include an isolated transistor in the present test device pool, since a solo transistor, in general, does not produce a large disturbance when interacting with heavy ions [2, 3].

**Test Methods**

The analog devices were tested as follows. The test device was biased at a typical burn-in configuration – an example for OP-15 is shown in Fig. 2. This biasing configuration limited the output noise to about ±10 mV in the test laboratory environment. The disturbance (SEU) at the output of an analog device was usually a pulse (of either positive or negative polarity). A storage oscilloscope was used to observe the rise time, duration, amplitude, and polarity of the pulses (see Fig. 3). The waveform was stored in computer memory in order to facilitate off-line analysis. After the waveform study was completed, we used the pulse height discriminator and counter subsystem to determine the number of disturbances (SEUs) at specific discriminator levels. Once the number of upsets was obtained for a specific setting of the discriminator (threshold voltage and the polarity), the SEU susceptibility cross-section was calculated for each monoenergetic ion species (and for each exposure angle) as described elsewhere [4]. The other operational

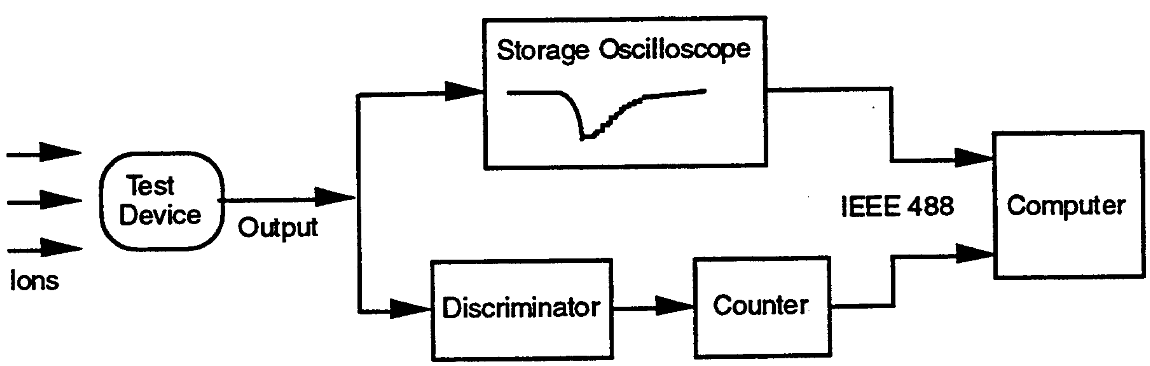


Fig. 3. Schematic representation of test equipment used to collect analog SEU data

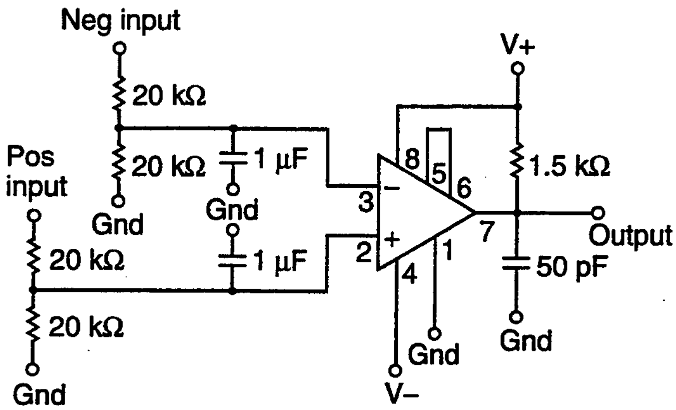


Fig. 4. Test circuit for LM111H comparator

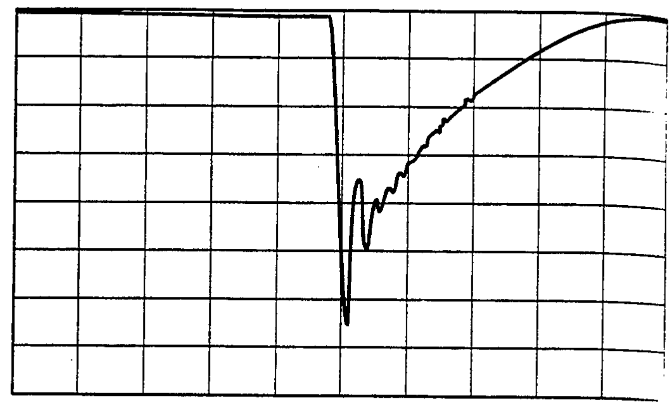


Fig. 5. LM111H pulse generated by a heavy ion

amplifiers were tested with a circuit very similar to that for OP-15; the LM111H comparator was tested using the test circuit shown in Fig. 4.

The SEU cross-section, σ, is defined, as for digital circuits, via the equation:

$$\sigma = \frac{N}{F \bullet \cos\theta}$$

where N is the number of upsets and ($F \bullet \cos\theta$) is the usual fluence/angle factor.

While the cross-section provides a convenient summary of the SEU susceptibility of digital devices, additional information is required to properly characterize the vulnerability of analog devices. This information should include the threshold voltage of the analog signal output, the pulse width, and the polarity of the disturbance.

### Test Results

A typical disturbance pulse (obtained with a xenon ion) for LM111H is shown in Fig. 5. The peak, lasting about 100 ns, was followed by a gradual trailing section lasting more than one microsecond. The peak was about -6.5 V (while the comparator was biased at ±15 V). The fine structure of the trailing edge was formed by the reflection of the main peak pulse. The initial pulse duration of 100 ns is long enough to trigger a digital circuit fabricated in almost any technology. When we counted such pulses using simple circuits consisting of a discriminator (set at -1 V) and a counter, we obtained the analog SEU cross-section curve shown in Fig. 6. The input voltage levels for LM111H are specified in order to describe the SEU susceptibility of the device in several test conditions. The bias voltage was ±15 V. The cross-section was relatively independent of the bias voltage levels from ±15 V down to ±10 V. We did not collect any data for bias voltage levels lower than ±10 V. Under these biasing conditions the output disturbances were predominantly negative going.

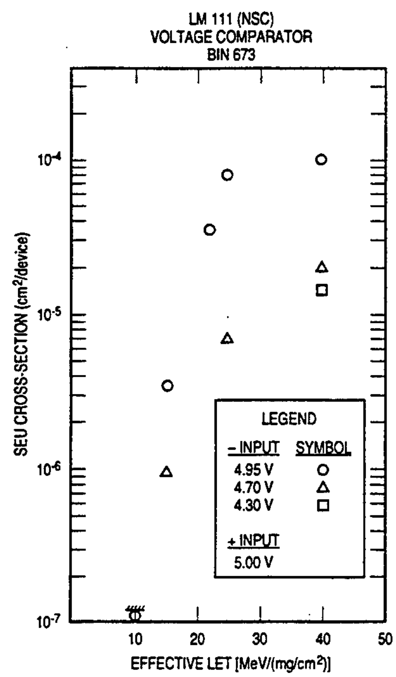


Fig. 6. Analog SEU cross-section curve for LM111H

The OP-15 operational amplifier produced both positive and negative SEU pulses. A pair of such pulses is shown in Fig. 7. In order to obtain the cross-sections for both polarities, we varied the voltage discriminator settings from ±50 to ±1000 mV. The dependence of the upset cross-section on the effective linear energy transfer (LET) of the beam is shown in Figs. 8 and 9, respectively, for positive and negative SEU pulses. As can be seen from the curves, the amplitudes of the pulses did not differ substantially for LETs above 15 MeV/(mg/cm²). The discriminator threshold voltage is therefore essentially independent of the cross-section, at least within this LET range. Most of the variations were due to statistical fluctuation of the discriminator pulse counts.

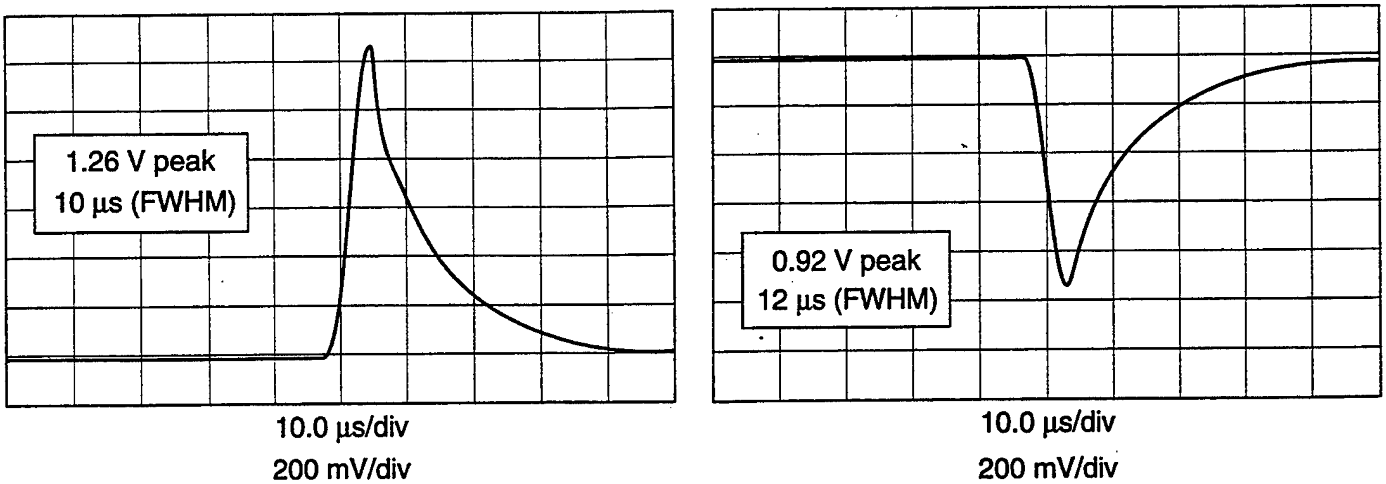


(a) Positive signal (1.3 V peak; 10µsec FWHM) (b) Negative signal (0.9 V peak; 12µsec FWHM)

Fig. 7. OP-15 output pulse generated by a xenon ion (±15V bias)

For OP-05 we obtained disturbances ranging from 30 to 800 mV, mostly limited to positive signals. A typical curve is shown in Fig. 10. The discriminator settings were 30, 100, 200, 400, 500, 600, 700, and 800 mV, as shown in Fig. 11. In contrast to OP-15, the different pulses varied in amplitude for OP-05; in particular, we obtained many more low amplitude pulses for OP-05 than for OP-15.

The HS3530RH often produced a waveform resembling a full sine wave, as shown in Fig. 12. Since the peak positive and negative amplitudes were essentially equal, only one cross-sectional curve, shown in Fig. 13, is reproduced here.

The four test device types differed in their SEU responses to heavy ions, as summarized in Table 2.

### Upset Mechanisms

Utilization of circuit simulations (such as SPICE) requires a detailed understanding of device layout characteristics. Unfortunately, our present effort to determine upset mechanisms has not been supported by the manufacturers of the devices. Therefore, our investigation of upset mechanisms has relied on: (1) information already available from the manufacturers' specifications, and (2) the utilization of a laser beam probe. While digital circuits have been investigated with laser beams in the past [5], a laser probing of analog devices has not previously been reported.

In this section we report the results of our laser investigation of OP-15 and OP-05, followed by a cursory description of upset mechanisms for HS3530RH and LM111H, obtained without the benefit of a laser probe.

#### *OP-15 and OP-05*

The saturation SEU cross-sections for OP-15 and OP-05 are about $2 \times 10^{-3}$ and $7 \times 10^{-4}$ cm$^2$ (measured with the discriminator setting at 200 mV), respectively, whereas the dies sizes are $2.5 \times 10^{-2}$ and $3.4 \times 10^{-2}$ cm$^2$. Therefore, the sensitive region in each die is but a fraction of the total die area. In order to identify the sensitive regions, we utilized an intensive laser beam available in our laboratory.

The laser excitation was performed with the output of a synchronously-pumped, cavity-dumped dye laser. The optical pulse width was about 15 picoseconds. The minimum laser spot size at the sample was about 1 µm$^2$. The laser wavelength was 600 nm. The optical absorption depth at this wavelength is about 1.8 µm. The optical intensity falls off exponentially into the

Table 2. Analog SEU Waveform Characteristics

| Device ID | Rise Time (nsec) | Width (FWHM in µsec) | Amplitude (mV) | Polarity |
|---|---|---|---|---|
| HS3530RH | 2500 | 3 | Up to 4000 | Positive & Negative |
| OP-05 | 2500 | 15 | Up to 800 | Mostly Positive |
| OP-15 | 3000 | 12 | Up to 1300 | Positive & Negative |
| LM111H | 100 | 0.5 | Up to 6000 | Mostly Negative |

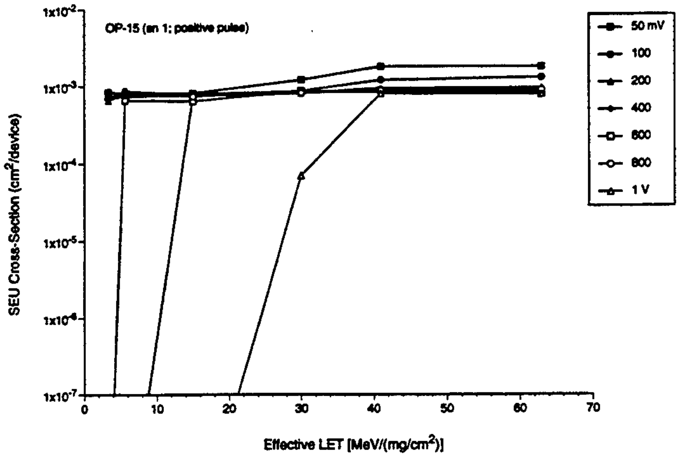


Fig. 8. OP-15 SEU cross-sections due to positive pulses

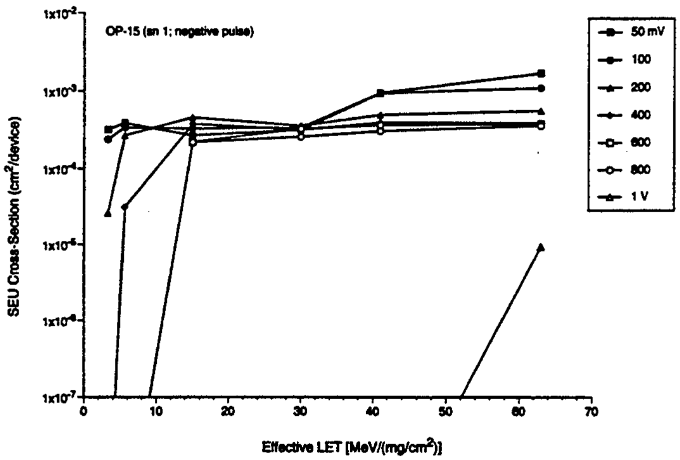


Fig. 9. OP-15 SEU cross-sections due to negative pulses

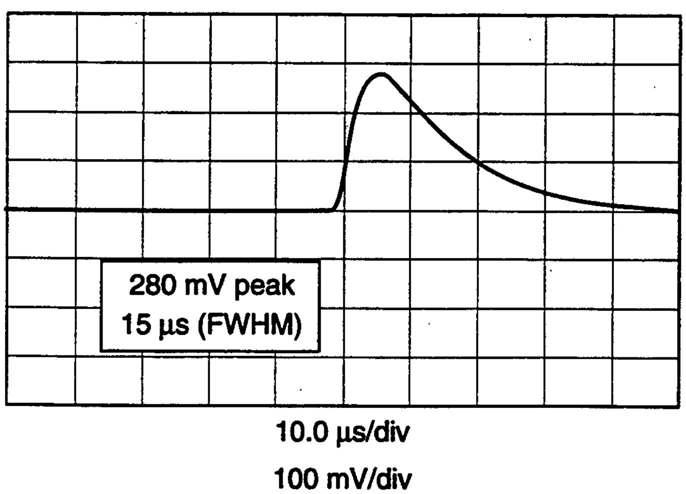


Fig. 10. OP-05 pulse generated by a heavy ion

bulk. Substantial excitation continues over a distance of several absorption depths. The laser LET was estimated using a formula developed by Kim et al. [6].

The entire surface of the OP-15 die was irradiated with a laser probe of varying spot size while the output of the device was monitored for tell-tale signs of a disturbance pulse. Output pulses were observed from 13 laser induced SEU sensitive regions (see Fig. 14), as shown in Table 3. The pulse widths are on the order of 5 µsec (FWHM). However, the pulse height depended upon the laser beam intensity and was therefore variable. When a low intensity beam was used, positive pulses were observed from region 1 and negative pulses from region 2. As the beam intensity was raised, the output waveforms became rather complex, and will therefore not be described further.

Visual inspection of the die (Fig. 14) enabled us to identify several of these regions and their associated transistors, as shown in Fig. 1.

Table 3. Laser SEU Sensitive Regions for OP-15

| Region | Transistors | Area (x $10^{-4}$ $cm^2$) |
|---|---|---|
| 1 | J2 | 5.6 |
| 2 | J1 | 5.6 |
| 3 | Q8 | 1.3 |
| 4 | J4 | 2.0 |
| 5 | J3 | 2.0 |
| 6 | J8 | 1.5 |
| 7 | Twin of J8 | 1.5 |
| 8 | Q3 & Q4 emitters | 1.3 |
| 9 | J5 | 2.0 |
| 10 | Q1 & Q2 | 3.8 |
| 11 | R5 & R6 | 1.5 |
| 12 | J6 | 6.0 |
| 13 | Q24 | 1.3 |
| | Total: | 3.5 x $10^{-3}$ $cm^2$ |

The majority of the sensitive regions were at the front end of the operational amplifier and were made of JFETs. The size of each region sensitive to laser exposure was measured, as summarized in Table 3. The total sensitive area was about 3 x $10^{-3}$ $cm^2$, which is within a factor of two of the saturation SEU cross-section obtained with heavy ions. Since the size of vulnerable area for laser exposure seems to agree with that of the area for analog SEU, the JFETs in the first difference amplifier may also be the major source of heavy ion induced SEU.

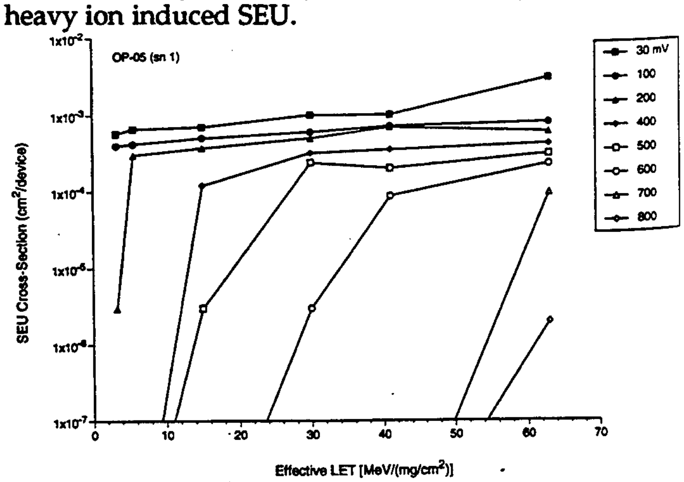


Fig. 11. SEU cross-sections for OP-05

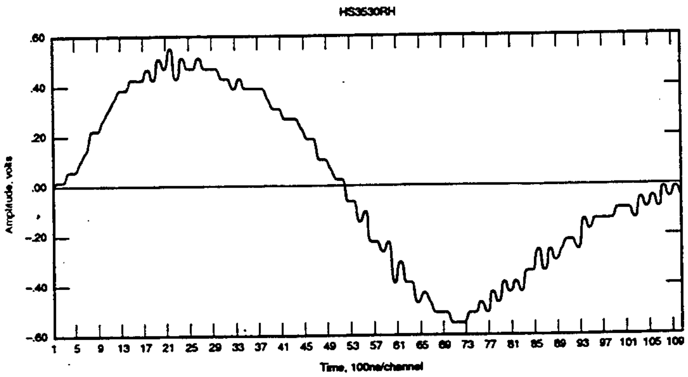


Fig. 12. HS3530RH output generated by a heavy ion

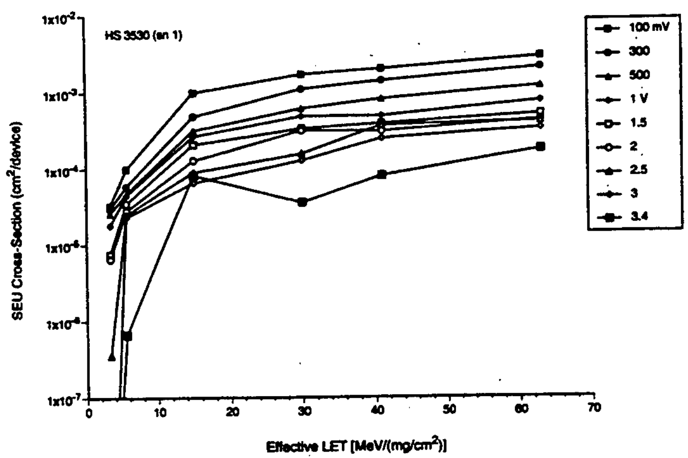


Fig. 13. SEU cross-sections for HS3530RH

Most of the area of the OP-05 die was tolerant of the laser beam irradiation, as shown in Fig. 15. A schematic circuit diagram for this device is reproduced in Fig. 16 to allow the identification of sensitive transistors within the die (this task has not been completed yet). The total sensitive area was 6 x $10^{-4}$ $cm^2$ (see Table 4), which is essentially the same as the saturation SEU cross-section measured with heavy ions. This agreement suggests that the vulnerable regions for heavy ions and laser beam exposure are the same.

Table 4. Laser SEU Sensitive Regions for OP-05

| Region | Transistors | Area (x $10^{-4}$ $cm^2$) |
|---|---|---|
| 1 | Q11 | 1.4 |
| 2 | Q12 | 1.4 |
| 3 | Q13 & Q14 | 0.3 |
| 4 | R6 | 0.5 |
| 5 | Q15 & Q18 | 2.4 |
| | Total: | 6.0 x $10^{-4}$ $cm^2$ |

Most analog circuits (including fast comparators and most operational amplifiers) have a very long recovery time (on the order of one microsecond) when the output voltage is driven to saturation. Figures 7 and 10 are indicative of such saturation. This suggests that, in some cases, the originally collected ionizing charge was amplified until the output voltage saturated.

*LM111H and HS3530RH*

We have not yet completed the laser beam studies for these device types. However, based on insights gained from our studies of OP-15 and OP-05, we expect that, for LM111H, a small amount of charge collected in the emitter in the front end or mid-section of the circuit can be amplified in the subsequent difference-amplifiers. A similar argument can be made for the HS3530RH operational amplifier.

## Discussion

Analog device outputs are often routed to digital circuits – possibly through a threshold detector, as is common in space electronics systems. An ionizing cosmic ray passing through an analog device can cause an analog SEU, which may then be propagated to, and stored within, the digital section of the circuit. It is suspected that such hybrid analog-digital SEUs have occurred in many space systems, including the TOPEX satellite (with OP-15). Hence, it is imperative that additional studies be initiated to investigate the general susceptibility of analog devices to SEU, with special consideration given to the interfaces between these devices and the systems in which they are embedded.

Ideally, each device type should be tested in a circuit that resembles the actual flight circuit; only then can the device's SEU response characteristics (including SEU pulse width, height, and polarity) be measured accurately. The effect of propagating analog SEUs to connected subsystems could also thereby be examined. However, in many cases the flight circuit may not lend itself to this type of simulation. We would therefore like to suggest that in order to more completely and clearly characterize the SEU susceptibility of an analog device the following information should (minimally) be provided: (1) test setup specification (materials and methods); (2) test circuit data, such as bias voltage; (3) an oscilloscope trace of the output disturbance; and (4) SEU cross-section curves. An oscilloscope trace is particularly important since it illustrates how the (possibly digital) connected circuit could be affected. Of interest here are the waveform, pulse height, rise time, duration, and polarity.

The impact of an analog SEU may be reduced by proper responses at the systems level. For example, the output of a voltage comparator should be examined twice before assuming that an actual level change has

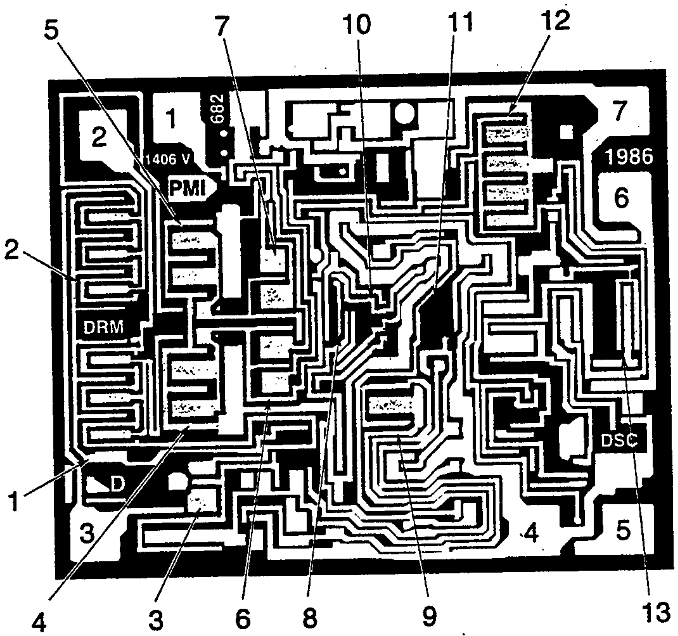


Fig. 14. Die layout for OP-15 operational amplifier
The die surface size is 1.73 x 1.42 mm. Pad designation is as follows: 1. balance; 2. inverting input; 3. non-inverting input; 4. V-; 5. balance; 6. output; 7. V+.

taken place, since it is possible to encounter an apparently stable level change caused by the momentary presence of a pulse due to an analog SEU. A second strategy, utilized on the TOPEX satellite, is to compensate for the occurrence of SEU by relaxing tolerance requirements. For example, if the output of an operational amplifier is connected to a counter, the flight computer could be instructed to tolerate extra counts due to analog SEUs. Thus, there are several strategies available at the systems level to help mitigate the impact of analog SEUs.

The study of analog SEUs is clearly in its infancy. Much work remains to be done to characterize the occurrence of these events and to develop mechanisms to overcome them. The present work is offered as a preliminary step towards these goals.

**Acknowledgments**

We gratefully acknowledge the Aerospace technical staff for the assistance in all phases of the testing procedure. We also would like to thank the LBL 88-inch cyclotron staff for beam delivery.

**References**

1. Gay C., Welch R., and Selby V., "Living with On-board Anomalies in the TOPEX/POSEIDON Earth Sensors," American Astronautical Society, Proceedings of the 16th Annual AAS Guidance Control Conference, AAS 93-044-1, Keystone, CO, February, 1993.
2. Wirth J.L., and Rogers S.C., "The Transient Response of Transistors and Diodes to Ionizing Radiation," IEEE Transactions on Nuclear Science, NS-11, No. 5, 24-38, 1964.
3. Long D.M., Florian T.R., and Casey R.H., "Transient Response Model for Epitaxial Transistors," IEEE Transactions on Nuclear Science, NS-30, 4131-4134, 1983.
4. Koga R., Kolasinski W.A., and Imamoto S., "Heavy Ion Induced Upsets in Semiconductor Devices," IEEE Transactions on Nuclear Science, NS-32, 159-162, 1985.
5. Buchner S.P., Wilson D., Kang K., Gill D., Mazer J.A., Raburn W.D., Campbell A.B., and Knudson A.R., "Laser Simulation of Single Event Upsets," IEEE Transactions on Nuclear Science, NS-34, 1228-1233, 1987.
6. Kim Q., Schwartz H.R., Edmonds L.D., and Zoutendyk J.A., "Diagnosis of NMOS DRAM Functional Performance as Affected by a Picosecond Dye Laser," Solid State Electronics, 35, 905-912, 1992.

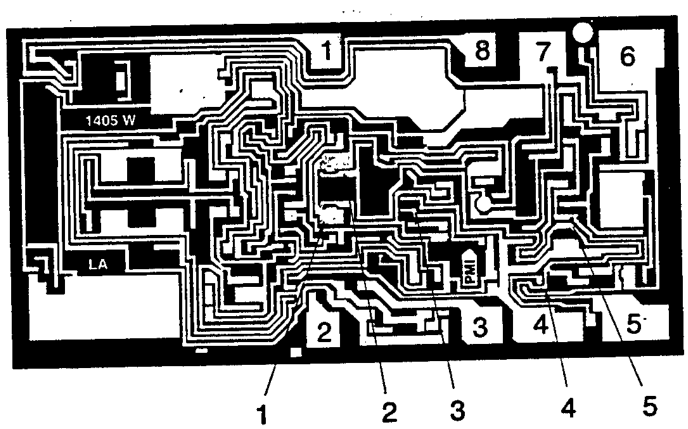


Fig. 15. Die layout for OP-05 operational amplifier
The die surface size is 2.54 x 1.32 mm. Pad designation is as follows: 1. balance; 2. inverting input; 3. non-inverting input,; 4. V-; 5. no connection; 6. output, 7. V+; 8. balance.

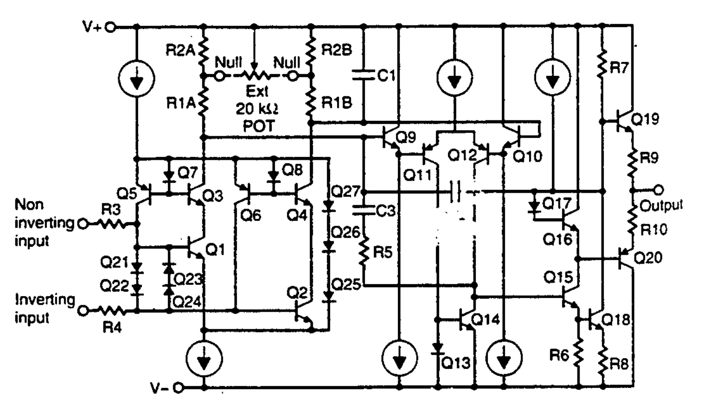


Fig. 16. Circuit schematic for OP-05 op amp
All transistors are bipolar type. Transistors Q1 through Q8 are used in the first difference-amplifier stage.

## TECHNOLOGY OPERATIONS

The Aerospace Corporation functions as an "architect-engineer" for national security programs, specializing in advanced military space systems. The Corporation's Technology Operations supports the effective and timely development and operation of national security systems through scientific research and the application of advanced technology. Vital to the success of the Corporation is the technical staff's wide-ranging expertise and its ability to stay abreast of new technological developments and program support issues associated with rapidly evolving space systems. Contributing capabilities are provided by these individual Technology Centers:

**Electronics Technology Center:** Microelectronics, VLSI reliability, failure analysis, solid-state device physics, compound semiconductors, radiation effects, infrared and CCD detector devices, Micro-Electro-Mechanical Systems (MEMS), and data storage and display technologies; lasers and electro-optics, solid state laser design, micro-optics, optical communications, and fiber optic sensors; atomic frequency standards, applied laser spectroscopy, laser chemistry, atmospheric propagation and beam control, LIDAR/LADAR remote sensing; solar cell and array testing and evaluation, battery electrochemistry, battery testing and evaluation.

**Mechanics and Materials Technology Center:** Evaluation and characterization of new materials: metals, alloys, ceramics, polymers and composites; development and analysis of advanced materials processing and deposition techniques; nondestructive evaluation, component failure analysis and reliability; fracture mechanics and stress corrosion; analysis and evaluation of materials at cryogenic and elevated temperatures; launch vehicle fluid mechanics, heat transfer and flight dynamics; aerothermodynamics; chemical and electric propulsion; environmental chemistry; combustion processes; spacecraft structural mechanics, space environment effects on materials, hardening and vulnerability assessment; contamination, thermal and structural control; lubrication and surface phenomena; microengineering technology and microinstrument development.

**Space and Environment Technology Center:** Magnetospheric, auroral and cosmic ray physics, wave-particle interactions, magnetospheric plasma waves; atmospheric and ionospheric physics, density and composition of the upper atmosphere, remote sensing, hyperspectral imagery; solar physics, infrared astronomy, infrared signature analysis; effects of solar activity, magnetic storms and nuclear explosions on the earth's atmosphere, ionosphere and magnetosphere; effects of electromagnetic and particulate radiations on space systems; component testing, space instrumentation; environmental monitoring, trace detection; atmospheric chemical reactions, atmospheric optics, light scattering, state-specific chemical reactions and radiative signatures of missile plumes, and sensor out-of-field-of-view rejection.